Effect of metal films on the photoluminescence and electroluminescence of conjugated polymers

H. Becker, S. E. Burns, and R. H. Friend
Cavendish Laboratory, Madingley Road, Cambridge CB3 0HE, United Kingdom
(Received 12 February 1997; revised manuscript received 15 April 1997)

We report the modification of photoluminescence (PL) and electroluminescence (EL) from conjugated polymers due to the proximity of metal films. The presence of a metal film alters the radiative decay rate of an emitter via interference effects, and also opens up an efficient nonradiative decay channel via energy transfer to the metal film. We show that these effects lead to substantial changes in the PL and EL quantum efficiencies and the emission spectra of the polymers studied here [cyano derivatives of poly(*p*-phenylenevinylene), PPV] as a function of the distance of the emitting dipoles from the metal film. We have measured the PL quantum efficiency directly using an integrating sphere, and found its distance dependence to be in good agreement with earlier theoretical predictions. Using the spectral dependence of the emission, we have been able to investigate the effect of interference on the radiative rate as a function of the wavelength and the distance between the emitter and the mirror. We compare our results with simulations of the radiative power of an oscillating dipole in a similar system. From our results we can determine the orientation of the dipoles in the polymer film, and the branching ratio that gives the fraction of absorbed photons leading to singlet excitons. We propose design rules for light-emitting diodes (LED's) and photovoltaic cells that optimize the effects of the metal film. By making optimum use of above effects we have substantially increased the EL quantum efficiencies of PPV/cyano-PPV double-layer LED's. [S0163-1829(97)09228-X]

I. INTRODUCTION

Conjugated polymers have attracted much attention since the discovery that these materials can be used as emissive layers in light emitting diodes (LED's).[1,2] Research has been particularly focused on poly(*p*-phenylenevinylene) (PPV) and its derivatives because of their high efficiencies. With these materials a wide range of emission colors and electroluminescence efficiencies up to 4% have been reported.[3] The competition between radiative and nonradiative decay processes in conjugated polymers is currently of great interest since it governs the efficiency of light emission in conjugated polymer devices such as LED's and lasers as well as the quantum yield of photovoltaic devices.[1,4–7] Most of these devices contain metals films either as electrodes for charge injection in electroluminescent devices or as mirrors in order to manipulate the radiative properties of the emissive species in the polymer. The presence of a metal film will always influence the properties of the emitting material. Microcavities have been used to narrow the linewidth and tune the color of emission from conjugated polymers.[8–10] It has recently been shown that the spontaneous emission rate can be greatly enhanced or suppressed in metal mirror microcavity structures containing conjugated polymers, depending on the overlap of the electric-field distribution within the microcavity with the emissive layer.[11,12] It has also been demonstrated that enhancement of the stimulated emission rate leading to lasing can be achieved with conjugated polymers using similar microcavity structures.[7]

More generally, the radiative and nonradiative rates of an excited dipole fluorescing in front of a metal film or between two metal films have been extensively investigated, both theoretically and experimentally.[13–20] The luminescence lifetime τ is related to the rate constants for radiative (k_R) and nonradiative (k_{NR}) decay by

$$\frac{1}{\tau} = k_R + k_{\mathrm{NR}}, \tag{1}$$

where the radiative lifetime is $1/k_R$, and the nonradiative lifetime is $1/k_{\mathrm{NR}}$. The quantum efficiency for luminescence q is given by

$$q = b\left(\frac{k_R}{k_R + k_{\mathrm{NR}}}\right), \tag{2}$$

where the branching ratio b is the fraction of absorbed photons leading to singlet excitons. The balance between the radiative and the nonradiative decay rates therefore determines the luminescence efficiency. Different methods have been used to predict the lifetime and luminescence quantum efficiency for an excited molecule in front of a mirror. The interference method successfully predicts the effects of a reflective surface on the radiative properties of the dipole.[15] However, at short distances nonradiative energy transfer to the metal becomes an effective decay channel for an excited molecule near a metal, thus increasing the nonradiative decay rate close to the metal. In the ''mechanical model''[14] the excited molecule is considered as a harmonic oscillator with the field reflected by the metal film acting as a driving force on the oscillator. By introducing a reflection coefficient smaller than unity and a phase factor into the perfect mirror equations, some of the aspects of nonradiative energy transfer could be reproduced.[14] However, the best agreement between theory and experiment has been achieved with the energy flux method where the total energy flux through infinite planes above and below the dipole is calculated.[19] It gives separate expressions for the effects of interference on the radiative lifetime and of nonradiative energy transfer on the nonradiative lifetime. The nature of the nonradiative energy transfer depends on the distance of the oscillating dipole

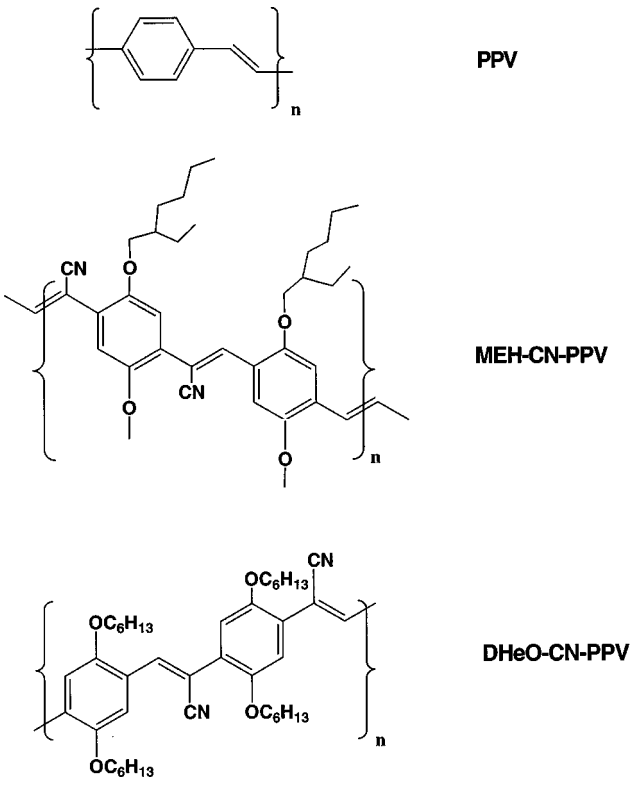

FIG. 1. Chemical structures of PPV, MEH-CN-PPV, and DHeO-CN-PPV.

to the metal. The interaction of the dipole with the electron gas of the metal is dominated by scattering by the metal surface at short (<20 nm) distances and scattering in the bulk, e.g., by phonons or impurities, for longer distances.[21,22] The decay time of an emitting molecule in front of a metal film has previously been reported.[15,19,23] In order to deduce the quantum efficiency from those measurements it was necessary to make assumptions about the orientation of the dipoles and the free-space efficiency of the emitting molecule. In this paper we present direct measurements of the photoluminescence (PL) and electroluminescence (EL) quantum efficiencies of two cyanoderivatives of poly(*p*-phenylenevinylene), MEH-CN-PPV and DHeO-CN-PPV, the structures of which are shown in Fig. 1, and compare our results with the theoretical predictions for the quantum efficiency of a dipole in front of a mirror. Measurements of the PL quantum efficiency rather than the luminescence lifetime are of particular relevance for electroluminescent devices.

The effect of interference on the radiative properties of an excited molecule is dependent on the emission wavelength. This wavelength dependence is again a function of the distance between the emitting molecule and the mirror. For broad bandwidth emitters such as conjugated polymers, this leads to substantial changes in the shape of the emission spectrum depending on the separation between the emitter and the mirror. We have investigated the changes in the PL emission spectrum of a 15–20-nm-thick MEH-CN-PPV film separated by a SiO_2 layer from a 35-nm-thick aluminium film. Using a simple model that describes the effects of interference on the radiative rates, we have been able to relate the spectral shape of the emission to the radiative power of an oscillating dipole in front of a mirror as a function of wavelength and distance between the polymer and the metal. We compare our results with earlier[24] and recent simulations of the radiative power of an emitting dipole in front of a metal mirror.

The internal electroluminescence efficiency of a LED is defined as the number of emitted photons per charge carrier flowing through the circuit. Because the light-emitting species is thought to be the same in EL and PL, we expect the effects of a metal film on the EL to be the same as measured for the PL. The maximum EL efficiency of a device is expected to be one-fourth of the PL efficiency of the emitting polymer where the factor 4 derives from the spin degeneracy of the singlet and triplet excitons, with only the singlet excitons decaying radiatively.[25] So far, the highest EL efficiencies for polymer LED's have been achieved with PPV/MEH-CN-PPV and PPV/DHeO-CN-PPV double-layer devices.[3,26] This has been attributed to various reasons, but it has been unclear what role interference effects and nonradiative energy transfer to the metal electrode play. In these devices it has been proposed that emission occurs from a thin layer at the interface between the polymer layers, although there has been little direct evidence that this is the case. We have systematically changed the position of the interface between the two polymer layers relative to the metal film. We measured the dependence of the EL efficiency of PPV/MEH-CN-PPV double-layer devices on the distance between the polymer-polymer interface and the Al electrode. This allows us to comment on the effect of the Al film on the radiative and nonradiative properties of the emitting species and the increased EL efficiencies in double-layer devices. We compare the EL efficiencies with the PL efficiencies measured on thin polymer films separated from a 35-nm Al film by a SiO_2 layer.

The interface between conjugated polymers and metals has recently been studied in order to obtain information about the chemistry that occurs at the interface and about diffusion of metal atoms into the near-surface region of the polymer.[27] The effects of these processes on PL and EL are important for device operation. It has also been reported that thin calcium films efficiently quench the PL of thin conjugated polymer films if deposited on top of them.[28] In this context it is important to understand the origin and consequences of nonradiative energy transfer from the polymer to the metal and of interference effects on the quantum efficiency and the emission spectrum.

II. METHOD

A. Experimental procedures

We have built three device structures as shown schematically in Fig. 2. Thin metal films of Al or Au were thermally evaporated onto one-half of a quartz substrate. We used semitransparent Al and Au films of thicknesses around 2–3 nm with a transmittance of more than 70% in the visible, and 35-nm-thick nontransparent Al films. Films of MEH-CN-PPV and DHeO-CN-PPV (Fig. 1) were prepared by spin coating onto the metal-coated substrates. A series of thicknesses between 15 and 200 nm was prepared. On a second set of samples, transparent SiO_2 spacer layers (Schott glass 8329) of differing thicknesses were evaporated on top of the metal-film coated substrates using an electron-beam evapo-

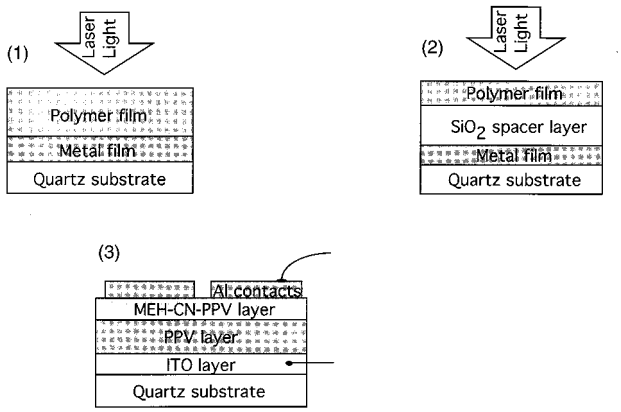

FIG. 2. Schematic diagram of the PL (1,2) and EL (3) device structures.

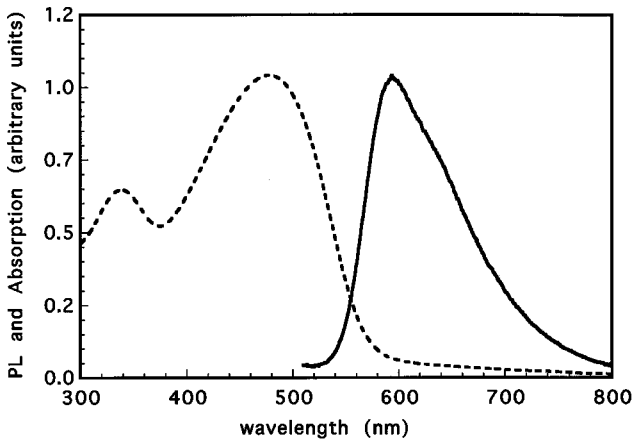

FIG. 3. Normalized emission spectrum (solid line) and absorption spectrum (dotted line) of MEH-CN-PPV.

ration technique. The refractive index of the glass was taken to be 1.47. A thin polymer layer of 15–20-nm thickness was then spin coated onto the SiO_2 layer. In order to investigate the effect of indium-tin oxide (ITO) on the PL quantum efficiency MEH-CN-PPV films of different thicknesses were spin coated onto commercially-available ITO-coated glass substrates (Balzers ITO-coated glass substrates type 257; ITO layer thickness $\sim$100 nm).

The PL efficiency (number of photons emitted per number of photons absorbed) and the emission spectra of the PL samples (structures 1 and 2, Fig. 1) were measured using an integrating sphere and a charge-coupled device (CCD) array spectrometer (Oriel Instaspec IV).[29,30] A 458-nm laser served as the excitation source. The samples were illuminated from the polymer side. The PL efficiency and the PL spectrum were measured on the metal-coated half, and as a reference on the noncoated half of the sample as a function of the thickness of both the polymer film and the SiO_2 layer.

A series of PPV/MEH-CN-PPV double-layer LED devices was built by spin-coating the PPV precursor onto ITO coated substrates. After thermal conversion of the PPV precursor, MEH-CN-PPV was spin coated onto the PPV film. Finally, Al electrodes were thermally evaporated on top of the structure. The PPV layer was 120 nm thick. The thickness of the MEH-CN-PPV layer varied between 24 and 110 nm. A schematic diagram of the devices is shown in Fig. 1. The electroluminescence in the forward direction was measured using a calibrated photodiode.

The batches of MEH-CN-PPV and DHeO-CN-PPV used showed PL quantum efficiencies between 33% and 39% when spin coated onto glass substrates. These are similar to those reported previously.[29] The samples were kept in a nitrogen-filled atmosphere or in vacuum at all times, and the experiments were performed within a few hours after the preparation of the samples in order to avoid oxidation of the polymer or the metal.

B. Modeling

Simulations of the radiative power of oscillating dipoles embedded in the top layer of a three-layer structure similar to structure 2 shown in Fig. 2 were carried out using the transfer-matrix method and multilayer stack theory. The model is based entirely on classical electromagnetic theory, and is described in more detail in Ref. 24. We simulated the radiative power of dipoles distributed uniformly throughout a 20-nm-thick layer separated from a 35-nm Al film by a transparent layer with the same refractive index as the SiO_2 that was used to build structure 2. The radiative power of the dipoles was normalized to be 1 in free space. By integrating the emitted power over all angles, the changes in radiative rate due to the metal film were calculated as a function of the distance between the emission layer and the metal, the wavelength and the orientation of the dipoles. The refractive index data for the aluminum was taken from Ref. 31. The refractive index of MEH-CN-PPV was taken to be 1.7, where any birefringence and the dispersion of the refractive index was neglected. The refractive index of MEH-CN-PPV at 633 nm has been measured to be 1.695 for TM and 1.77 for TE modes.[32]

III. RESULTS

A. PL spectra and PL efficiency

The PL emission and absorption spectra of MEH-CN-PPV are shown in Fig. 3. Due to the large Stokes' shift typical of this class of materials, the overlap between absorption and emission is very small. For wavelengths above 550 nm this allows us to use the spectra measured in the integrating sphere, since reabsorption of the emitted light is low and the shape of the emission spectrum is therefore the same as for the free-space emission.

1. Polymer on metal (structure 1)

Figure 4 shows the PL efficiency of MEH-CN-PPV and DHeO-CN-PPV films in front of different metal films as a function of the film thickness. 2- and 3-nm-thick gold and aluminum films were used as well as 35-nm-thick aluminium films. The data were corrected for the absorption of laser light by the metal mirror, which was calculated from the transmission spectra of the metal films, simulations of the absorption of light by the metal,[33] the transmission spectra of the polymer films, and the absorption by the whole structure measured in the integrating sphere. The 2–3-nm-thick metal films are highly transparent for light in the visible range ($>$70% transmittance). Hence we expect interference effects

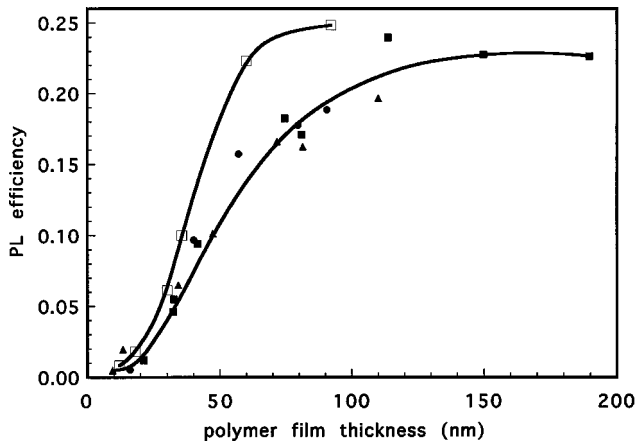

FIG. 4. PL quantum efficiency as a function of the polymer film thickness of MEH-CN-PPV on 2 nm of gold (triangles), MEH-CN-PPV on 3 nm of aluminium (circles), DHeO-CN-PPV on 2 nm of gold (filled squares) and of MEH-CN-PPV on 35 nm of aluminum (open squares). The solid lines are guides to the eye.

to play a minor role. Figure 5 shows the spectra measured in the integrating sphere for MEH-CN-PPV films of different thicknesses on 3 nm of Al.

We measured the absorption coefficient for the MEH-CN-PPV at 458 nm to be $\alpha = 1.24 \times 10^5$ cm^{-1}, so that approximately half of the excitation light is absorbed in the first 56 nm. Since the diffusion range for the excitons in these materials is of the order of a few nanometers, we take the spatial distribution of the emission to be identical to the absorption profile. For thick polymer films, where most of the light is emitted in regions far away from the metal, the shape of the emission spectrum is the same as for thin films, where the light is emitted close to the metal. This confirms that interference effects are negligible for 2–3-nm-thick metal films. We see from our measurements that the PL is efficiently quenched for polymer films up to a thickness of 90 nm for thin metal films, and up to 60 nm for a thick Al film. Within a critical distance of 20 nm almost all luminescence is quenched.

Figure 4 also shows the dependence on the polymer film thickness of the PL quantum efficiency of MEH-CN-PPV

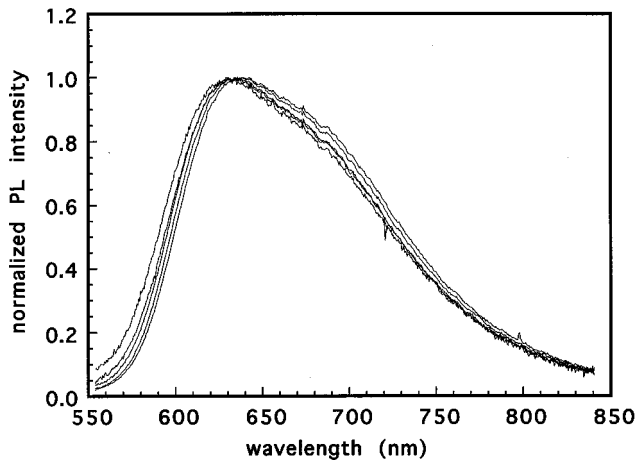

FIG. 5. Normalized PL emission spectra of 15–90-nm-thick MEH-CN-PPV films on 3 nm of aluminum measured in the integrating sphere.

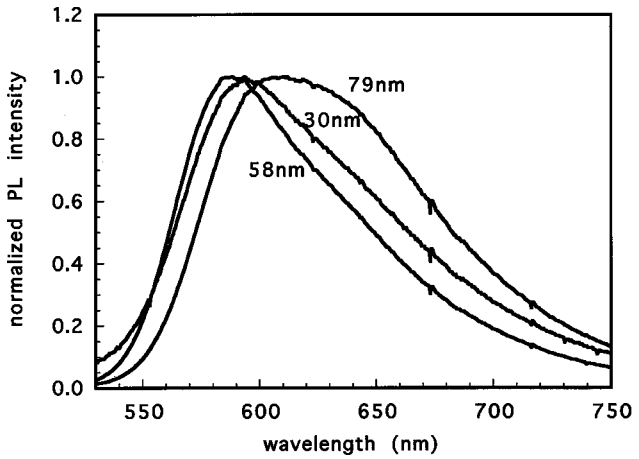

FIG. 6. Normalized PL emission spectra of three selected thicknesses of MEH-CN-PPV films on 35 nm of aluminum measured in the integrating sphere.

films deposited on 35 nm of Al. The reflectance of the metal film was around 90%. As shown in Fig. 6, the shape of the emission spectrum changes with the polymer film thickness due to interference effects. Surprisingly, the PL quantum efficiency rises faster with polymer film thickness than for thin metal films. The difference in the distance dependence of the energy transfer rate to the metal cannot explain this. However, interference effects not only affect the emission properties of a material but also change the absorption in the same fashion. As we will see in Sec. III A 2, the radiative power of dipoles parallel to the mirror plane increases with the distance between the mirror and the dipole for distances comparable to the maximum MEH-CN-PPV film thickness. We therefore expect the absorption of light to increase with distance from the metal. The majority of light is therefore absorbed and emitted further away from the metal than in the case of thin metal films with a low reflectivity. As a consequence, the maximum PL efficiency is reached for thinner polymer films.

The same experiment was performed with polymer films of differing thicknesses spin-coated on ITO-coated glass substrates. ITO, which is commonly used as a hole injector in electroluminescent devices, was not found to quench the PL for polymer films thicker than 20 nm. Only for a 20-nm-thick film was a reduction of the PL efficiency of 12% observed. This might be explained in terms of exciton diffusion toward the polymer-ITO interface where the excitons are quenched. Our results are in agreement with reports in the literature.[28,34,35]

Discussion. The suppression of light emission near the polymer metal interface cannot be explained by absorption of emitted light by the metal. Although this effect reduces the measured quantum efficiency, it is independent of the distance between the metal and the emitter, and can therefore not explain the increase in quantum efficiency with polymer film thickness. At long distances the PL efficiency approaches a constant value below the free-space quantum efficiency of our samples. As we will see below this is consistent with our assumption that interference effects can be neglected for very thin metal films. Our data agree qualitatively with a calculation of the quantum yield of an oscillating dipole with a quantum efficiency of unity in front of a

mirror.[19] We conclude that nonradiative energy transfer from the excited state of the polymer to the metal efficiently quenches luminescence in the proximity of a metal film, as predicted by the simulations by Chance, Prock, and Silbey.[19]

However, for three reasons our results are not directly comparable with the calculation of Chance, Prock, and Silbey. First, in their model, the quantum efficiency of a single dipole at a given distance is calculated. In our experiments the light is emitted over a broad region in the polymer film depending on where it is absorbed. Even for thick polymer films light penetrates far into the film, where it is absorbed and subsequently emitted in regions close to the metal where it can be quenched. Because of the penetration of light into the polymer film we expect a reduction in the quantum efficiency for relatively thick polymer films. Second, Chance, Prock, and Silbey, used a model in which the emitter had a quantum yield of unity in free space. It follows that in free space no nonradiative energy decay occurs. Energy transfer to the metal is therefore the only nonradiative decay channel. This means that interference effects do not change the quantum efficiency for distances where nonradiative energy transfer to the metal is negligible. They do, however, alter the quantum efficiency at short distances where nonradiative energy transfer to the metal is present. In our structures, shown in Figs. 4–6, interference effects alter the PL efficiency at all distances when the reflectivity of the metal films is high, since our materials have a free-space quantum efficiency around 36%, and therefore intrinsic nonradiative decay channels not associated with the metal film are present. However, interference is negligible for all distances when the reflectivity of the metal films is low. Third, highly transparent metal films show a slightly different distance dependence of the nonradiative energy-transfer rate than thick metal films. At short distances very thin films quench luminescence more efficiently than thick metal films, whereas for longer distances the opposite is true.[18]

2. Polymer on spacer on metal (structure 2)

We also investigated the PL efficiency and the emission spectra of structures where a 20-nm-thick polymer layer is separated from the Al film by a SiO_2 space layer. Using spacer layers avoids several problems. The emission zone is confined to a thin layer at a given distance to the metal, which gives better spatial resolution and allows better comparison with simulations for dipoles in front of metal films.[15,19,24] It avoids chemical reactions between the polymer and the metal that can alter the emission characteristics of the polymer, e.g., covalent bonding of Al atoms to the polymer.[27] It also rules out diffusion of the exciton to the metal as a necessary precondition for quenching. Furthermore, no diffusion of metal atoms into the polymer layer [of the order or 3–4 nm for Al (Ref. 27)] occurs. In addition, a comparison of the EL results with the PL quantum efficiency of a polymer film at various distances to the metal allows us to draw conclusions about the nature of the recombination zone. The measured quantum efficiencies were corrected for the absorption of laser light by the Al film.

In Fig. 7 the PL quantum efficiency of a 15–20-nm-thick polymer film separated from 2–3-nm-thick Au and Al films by a transparent SiO_2 spacer layer is shown as a function of the spacer layer thickness. For a polymer film spin coated directly onto the metal film or a 5-nm-thick spacer layer, the efficiency is reduced from 36% in free space to a value between 0.06% and 3%. We note that contact between the polymer film and the metal is not necessary for efficient quenching of the PL. The PL quantum efficiency increases with increasing SiO_2 layer thickness. For a separation of approximately 60 nm, the PL quantum efficiency approaches a constant value which is less than the free-space quantum efficiency of 36%. The excitation density throughout such a thin film is taken to be approximately constant. For our samples we therefore consider 60 nm as the distance above which nonradiative energy transfer to the metal becomes negligible. The PL spectra obtained from the polymer films are shown in Fig. 8. As expected, for highly transparent metal films the shape of the emission spectrum is almost independent of the distance between the polymer layer and the metal film.

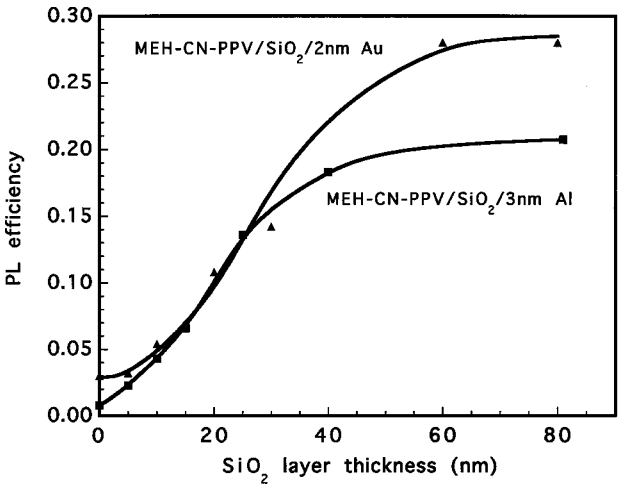

FIG. 7. PL quantum efficiency of a 15–20-nm-thick MEH-CN-PPV film on a SiO_2 spacer layer on 2 nm of gold or 3 nm of aluminum as a function of the SiO_2 thickness. The solid lines are guides to the eye.

Figure 9 shows the results of the same measurement on samples with a 35-nm-thick highly reflective Al film. The

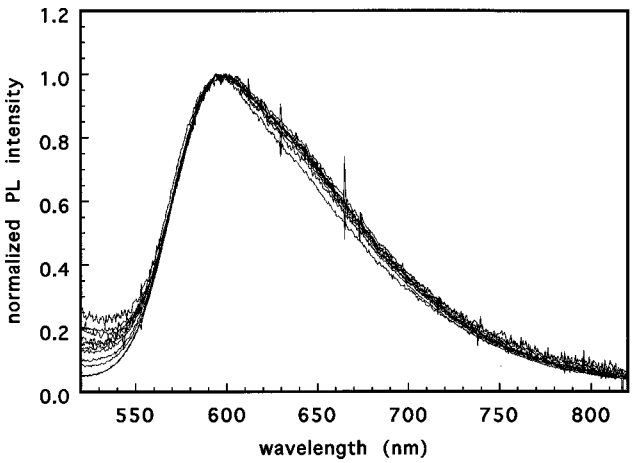

FIG. 8. Normalized PL emission spectra of 15–20-nm-thick MEH-CN-PPV films separated by SiO_2 spacer layers of different thicknesses from 2 nm of gold and 3 nm of aluminum measured in the integrating sphere.

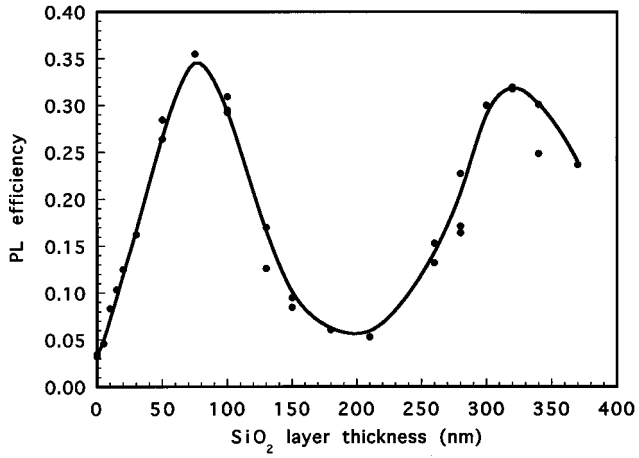

FIG. 9. Solid circles: PL quantum efficiency of a 15–20-nm-thick MEH-CN-PPV film on a SiO_2 spacer layer on a 35 nm of aluminum as a function of the SiO_2 thickness. The solid line is a guide to the eye.

reflective and quenching properties of such an Al film are identical to that of the bulk. The PL quantum efficiency oscillates as a function of the SiO_2 layer thickness. With no spacer layer present, the PL quantum efficiency is again reduced to around 3%. With increasing SiO_2 layer thickness the quantum efficiency rises to a maximum of 35.5% for a separation of about 75 nm between the polymer layer and the metal film. For larger distances, the PL is significantly reduced, with the quantum efficiency dropping to 5.3% for a SiO_2 layer of 210-nm thickness. The PL quantum efficiency peaks again, with the quantum efficiency reaching 32%, a value slightly lower than that for the first peak. We note that the PL quantum efficiencies shown in Fig. 9 have been calculated neglecting the absorption of emitted light by the Al. Correction for absorption of PL by the Al would give a maximum PL quantum efficiency of 37%, and a minimum PL quantum efficiency of 5.6%, as discussed below. The PL spectra from these samples are shown in Fig. 10. Interference effects shift the emission peak of a thin MEH-CN-PPV layer on top of a SiO_2 spacer and a 35-nm-thick Al film over the

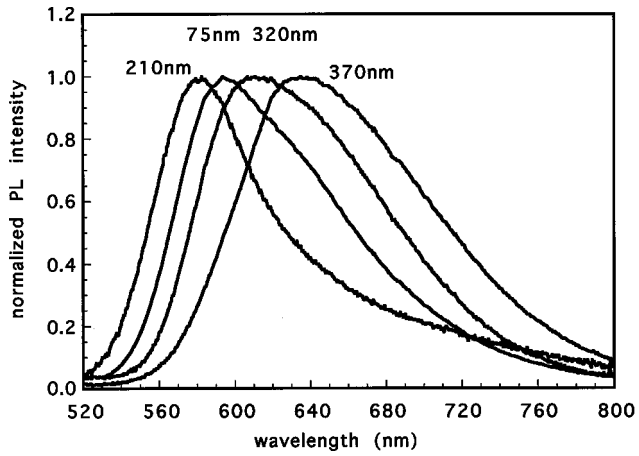

FIG. 10. Normalized PL emission spectra of 15–20-nm-thick MEH-CN-PPV films separated by SiO_2 spacer layers of four selected thicknesses from 35 nm of aluminum measured in the integrating sphere.

range of 580–640 nm. The emission from a MEH-CN-PPV film spin coated onto a glass substrate peaks at 595 nm.

Discussion. In our experiments we can distinguish between two cases. For very thin metal films with low reflectivities, interference effects are negligible. This is supported by the lack of any dependence of the shape of the emission spectrum on the thickness of the polymer film or the SiO_2 spacer layer. Nonradiative energy transfer to the metal has, however, been identified as an efficient decay channel for an emitter in the proximity of a thin metal film.[19,22] The samples with thin metal films thus allow us to measure the effect of the metal film on the nonradiative energy transfer only and to neglect the effect of interference on the radiative rate. For thick metal films we expect both interference effects and energy transfer to the metal to influence the radiative as well as the nonradiative properties of the light emitter.[14,15,19]

We can identify two different regimes. For short distances (below 60 nm) we see efficient quenching of the luminescence for both highly transparent and highly reflective metal films. We conclude that nonradiative energy transfer to the metal plays an important role in this region. For longer distances the PL efficiency remains constant for polymer films on thin metal layers but oscillates as a function of distance for highly reflective metal films. For thicker metal films we also observe a significant dependence of the shape of the emission spectrum from the distance between the emitter and the metal. We assign these effects to interference between directly emitted waves and waves reflected from the metal layer. The effect of interference on the radiative lifetime of an emitting dipole in front of a metal mirror as a function of wavelength and dipole metal separation has been investigated in great depth,[15,23] and, as we discuss below, can account for our observations here.

In order to interpret our results, we have analyzed them in terms of the competition between radiative and nonradiative decay processes. The radiative lifetime of an excited molecule oscillates with increasing distance of the molecule from a reflective surface. However, when the nonradiative energy transfer to the metal is negligible, the radiative decay channels in a material with a quantum efficiency of unity do not compete with any nonradiative decay channels. Changes in the radiative lifetime therefore have no effect on the quantum efficiency. We note that this is the case for the simulations carried out in Ref. 19. If, however, nonradiative decay channels are present, as in our materials, an oscillation in the radiative lifetime due to interference effects will allow the nonradiative decay channels to compete more or less favorably, depending on whether the radiative lifetime is increased or decreased. This leads to an oscillation in quantum efficiency. For materials where radiative and intrinsic and extrinsic (i.e., due to the metal) nonradiative decay channels compete with each other, we therefore expect a combination of both the effects of interference on the radiative lifetime and of energy transfer to the metal on the nonradiative lifetime. At long distances we expect the PL efficiency to oscillate in the same fashion as the radiative lifetime (see Fig. 9). At short distances nonradiative energy transfer will reduce the efficiency (see Figs. 9 and 4). This effect will be enhanced by an increase in the radiative lifetime (decrease in the radiative rate) due to destructive interference.

Dipole orientation. The distance dependence of the radiative lifetime of a dipole in front of a reflective metal film is very sensitive to the orientation of the dipole. In the following we will summarize a few results of simulations by Chance, Prock, and Silbey of the quantum efficiency of a dipole with a free-space quantum efficiency of unity in front of a metal mirror. We introduce a normalized length $x = 2\pi nd/\lambda$ (where n is the refractive index of the medium surrounding the dipole, d is the distance, and λ is the wavelength at which the dipole emits). For dipoles parallel to the mirror, the radiative lifetime increases rapidly with decreasing distance between the dipole and the mirror. This is the case for distances for which x is less than 1. For $n=1.5$ and $\lambda = 600$ nm, parameters comparable with our experiment, x is 1 for a dipole-metal separation of 64 nm. For dipoles oriented perpendicular to the metal film the radiative lifetime shows a maximum around $x=1.7$, which for $n=1.5$ and $\lambda = 600$ nm gives a distance of around 100 nm.[15,19] This leads to significant differences in the distance dependence of the quantum efficiency. For parallel dipoles the quantum efficiency increases continuously with distance.[19] At a distance of $x=1$ the PL quantum efficiency is about 0.8. For perpendicular dipoles the peak in radiative lifetime at $x=1.7$ results in a dip in quantum efficiency because the nonradiative decay channels compete more favorably when the radiative rate is low. We note that in the region from $x=0.5-3$ (30–200 nm for the above parameters) the radiative rate for a dipole oriented perpendicular to the mirror is much smaller than for the parallel case.[19,24] This means that nonradiative energy transfer to the metal competes successfully with radiative decay for distances much longer than in the parallel case. The PL quantum efficiency for dipoles oriented perpendicular to the substrate will therefore be low for much larger distances than in the parallel case. High quantum efficiencies are only reached at long distances ($x>3$). For a perpendicular dipole with a free-space quantum efficiency of 1, a quantum efficiency of 0.5 is not reached until a distance ten times that for a parallel dipole.[19] A measurement of the quantum efficiency of a thin polymer layer in front of a reflective metal film as a function of the distance between the metal and the polymer therefore provides a sensitive means of measuring the orientation of the dipoles. Since the difference in the distance dependence of the PL quantum efficiency of perpendicular and parallel dipoles arises from interference effects, we will compare the simulations by Chance, Prock, and Silbey with our results for reflective Al films shown in Fig. 9. The PL quantum efficiency reaches a maximum of 85% of the free-space quantum efficiency when the dipoles are 75–95 nm away from the metal. This rapid increase is consistent with the majority of the dipoles being oriented parallel to the mirror. However, a quantitative analysis is only possible if the intrinsic nonradiative decay channels are included into the picture. We will return to this point in Sec. III B.

B. PL spectra and radiative emission rates

As seen in Figs. 6 and 10, the emission spectra change substantially with the distance between a reflective metal film and an emissive polymer film. We have already assigned this to interference between the directly emitted waves and the waves reflected from the metal mirror. Interference alters the radiative lifetime of the emissive species as a function of wavelength. The spectral shape and the magnitude of emission are then determined, respectively, by the changes in radiative rate and the competition between radiative and nonradiative decay processes.

The radiative lifetime and the radiative power of an oscillating dipole in front of a metal mirror as a function of wavelength and distance between the dipole and the mirror have been calculated previously.[14,15,19,23,24] Taking the natural oscillator strength of the transition (with the emitter in free space) and the competition between radiative and nonradiative decay processes into account, we relate the measured emission spectra (as shown in Fig. 10) to simulations of the radiative power of a dipole. In the following we perform a simple calculation that translates the emission spectra into the radiative power of a dipole in front of a mirror as a function of wavelength and distance between the dipole and the mirror. In the calculation we assume that all the emission comes from transitions from one excited state or from an ensemble of excited states which are very close in energy. In the latter case, either the states must all be coupled to the same ground state with approximately the same radiative rate, or energy transfer between them must be very fast and highly efficient. This assumption is justified by the fact that efficient channeling of all emission from several microcavity modes into a single mode has been observed in the case of lasing.[7]

The PL quantum efficiency is defined as in Eq. (2). The total radiative rate for the system can be written as the integral over the radiative rates of all transitions,

$$K_R = \int k_R(\lambda)\, d\lambda, \tag{3}$$

where $k_R(\lambda)d\lambda$ is the radiative rate for transitions at wavelengths between λ and $\lambda + d\lambda$. The PL quantum efficiency q_0 is given by

$$q_0 = \frac{K_R}{K_R + K_{\mathrm{NR}}} = \frac{\int k_R(\lambda)\, d\lambda}{\int k_R(\lambda)\, d\lambda + K_{\mathrm{NR}}}. \tag{4}$$

If the radiative rate is altered, for example, by interference effects due to a mirror, the new quantum efficiency q' is given by

$$q' = \frac{\int g(\lambda) k_R(\lambda)\, d\lambda}{\int g(\lambda) k_R(\lambda)\, d\lambda + K_{\mathrm{NR}}}, \tag{5}$$

where $g(\lambda)$ is a correction factor that accounts for the modification of the radiative rate as a function of wavelength. $g(\lambda)$ is equivalent to the function that describes the radiative power calculated for a dipole in front of a mirror as a function of wavelength, with the radiative power of the dipole in free space normalized to 1.

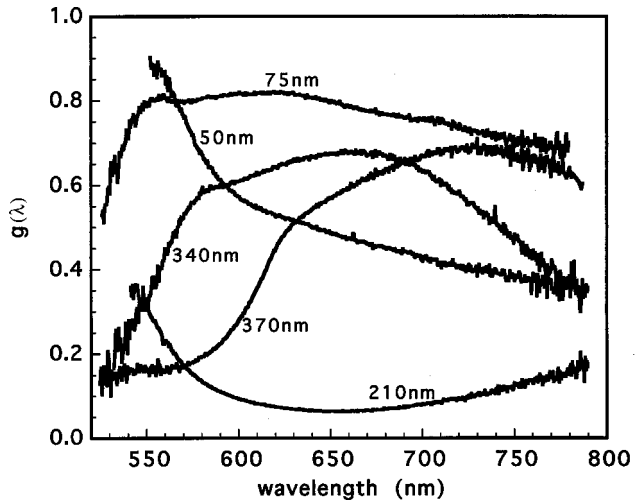

FIG. 11. $g(\lambda)$ as a function of wavelength for different SiO_2 layer thicknesses between the MEH-CN-PPV film and the 35-nm-thick aluminum film.

The free-space emission spectrum $S_0(\lambda)$, measured over all angles, is proportional to the ratio of the radiative rate for the transition with wavelength λ to the total decay rate ($K_R + K_{NR}$):

$$S_0(\lambda) \propto \frac{k_R(\lambda)}{\int k_R(\lambda)d\lambda + K_{NR}}. \tag{6}$$

The emission spectrum when modified by changes in the radiative rate, $S'(\lambda)$, is then given by

$$S'(\lambda) \propto \frac{g(\lambda)k_R(\lambda)}{\int g(\lambda)k_R(\lambda)d\lambda + K_{NR}}. \tag{7}$$

Dividing S' by S_0 and inserting Eqs. (4) and (5) yields

$$\frac{S'(\lambda)}{S_0(\lambda)} = g(\lambda)\left(\frac{1-q'}{1-q_0}\right). \tag{8}$$

This is an important result, since it allows us to calculate the changes in radiative rate $g(\lambda)$ directly from the measured emission spectra, given also values of q_0 and q' which are measured directly in the integrating sphere. We can also calculate the new spectrum $S'(\lambda)$ of an emitter that is moved into a new environment from the old emission spectrum, the quantum efficiencies and simulations of $g(\lambda)$ as described in Sec. II B. We calculated $g(\lambda)$ from Eq. (8) using the measured spectra and efficiencies for thin MEH-CN-PPV films separated by a SiO_2 spacer layer from a 35-nm-thick Al film (structure 2, Fig. 2). The spectra were normalized by the amount of excitation light absorbed by the polymer film. This correction is necessary since the absorption itself is a function of the distance between the polymer film and the metal (in the same fashion as the emission), as well as of the angle of incidence.[11] The total absorption in the device was corrected for the absorption of laser light by the Al film. $g(\lambda)$, as deduced from our experiments using Eq. (8), is shown in Fig. 11 at various values of the thickness of the SiO_2 spacer layer. In the above calculation the nonradiative rate is kept unchanged. It therefore only accounts for changes of the radiative rates, i.e., interference effects. For this reason only spectra of polymer films at distances of 50 nm or more from the metal were used for the calculation of $g(\lambda)$. Both the shape and magnitude of $g(\lambda)$ show a significant dependence on the distance between the polymer film and the metal layer. The shape of $g(\lambda)$ accounts for the changes in the emission spectra shown in Fig. 10, whereas the magnitude of $g(\lambda)$ explains the oscillation in PL efficiency shown in Fig. 9.

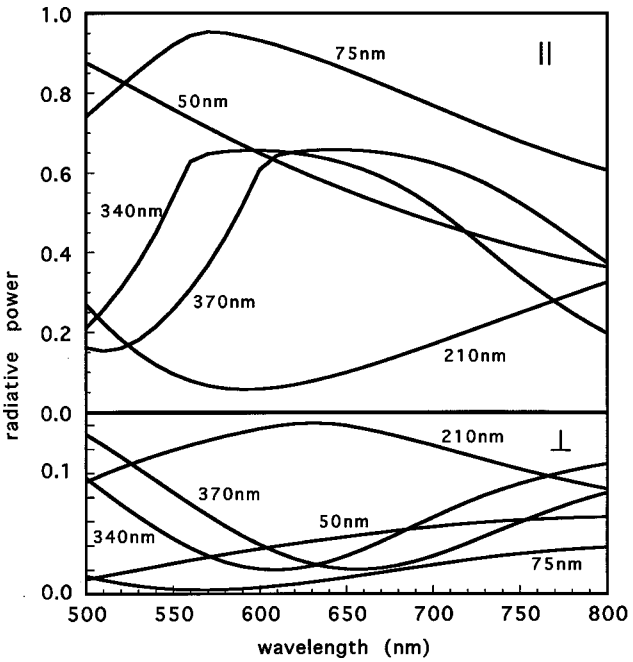

FIG. 12. Simulation of the radiative power of a 20-nm-thick film of dipoles with a radiative power of unity in free space as a function of wavelength and SiO_2 layer thicknesses between the dipoles and a 35-nm-thick aluminum film. The top and bottom graphs show simulations for dipoles oriented parallel and perpendicular to the metal film.

Figure 12 shows simulations of the radiative power (integrated over all angles) of a uniform distribution of dipoles in a 20-nm-thick layer separated from a 35-nm Al layer by a dielectric layer with the same refractive index as the SiO_2 that we used in our experiment. The method used is described in Ref. 24. The radiative power is shown for dipoles parallel and perpendicular to the metal films. In free space the radiative power of the dipoles is taken to be the same at all wavelengths, and the total radiative power of the dipoles is taken to be unity. The simulations therefore show the function $g(\lambda)$ for a set of dipoles distributed within a 20-nm-thick layer as a function of the distance between the dipoles and an Al film. Comparison between $g(\lambda)$ deduced from our spectra and $g(\lambda)$ for parallel dipoles as calculated above shows very good agreement between the two. It is important to note that our calculations include the effects of reflection from all interfaces in our structures as was found to be necessary in the work of Ref. 19. Figure 11 also shows that for a 75-nm-thick spacer layer, $g(\lambda)$ is constantly high in the wavelength region of emission. This is why the PL efficiency peaks for that distance, and why the emission spectrum is similar to that of the free-space emission. Again for a 340-

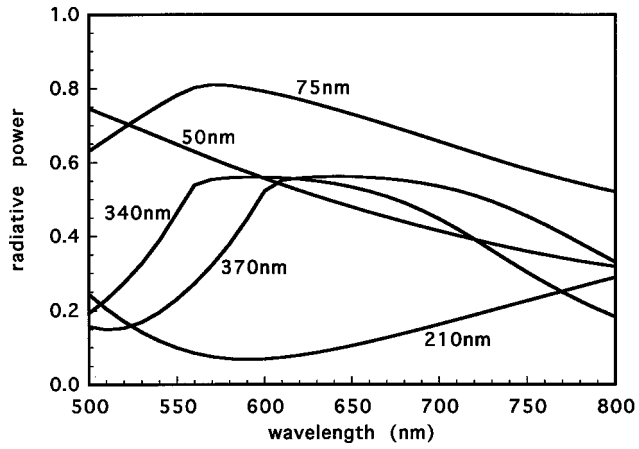

FIG. 13. Simulation of the radiative power of a 20-nm-thick film of dipoles with a radiative power of unity in free space as a function of wavelength and SiO_2 layer thicknesses between the dipoles and a 35-nm-thick aluminum film. 85% of the dipoles are oriented parallel and 15% perpendicular to aluminum film.

nm-thick spacer layer, $g(\lambda)$ is relatively high for wavelengths where MEH-CN-PPV emits, resulting in a second maximum in the PL quantum efficiency at that distance. Conversely, $g(\lambda)$ is very low for a 210-nm-thick spacer layer, leading to a minimum in PL quantum efficiency. We can also see that for a 370-nm-thick SiO_2 layer, $g(\lambda)$ shows large changes between 550 and 750 nm. It is low between 550 and 600 nm, suppressing emission in that spectral region. Between 620 and 750 nm, $g(\lambda)$ is high, encouraging emission above 620 nm. This leads to the large redshift for the emission from a MEH-CN-PPV film at a distance of 370 nm from the Al seen in Fig. 10. We conclude that interference effects sufficiently explain the changes in the emission intensity and the emission spectra seen in our devices for SiO_2 layer thicknesses above 50 nm, where nonradiative energy transfer to the metal becomes small.

The reflective Al surface not only changes the total power radiated by the dipoles, but also the angular distribution of emission. It is interesting to note that the maximum radiative power is not achieved for a structure that emits most of the light into the forward direction, but rather for a structure for which the maximum emission is directed at an angle approximately 30° off axis.

C. Dipole orientation and branching ratio

In Sec. III B we presented a successful model for the changes in the radiative rates and the emission spectra of a light-emitting polymer layer in front of a reflective Al film. In the following we will use this model to obtain more information about the orientation of the dipoles and the branching ratio b in our materials.

1. PL spectra and dipole orientation

Figures 12 and 13 show simulations of the radiative power of dipoles oriented parallel and perpendicular to the metal film, as well as a distribution of parallel and perpendicular dipoles. The shape of the curves is distinctively different for different orientations. Comparison of the simulated radiative power with $g(\lambda)$ as deduced from our measurements gives us a sensitive measurement of the orientation of the dipoles. The simulation for parallel dipoles qualitatively reproduces $g(\lambda)$, as deduced from the measured PL spectra. However, the radiative power calculated for parallel dipoles is too high for polymer-metal distances of 50, 75, 340, and 370 nm, and too low for a distance of 210 nm, in order to give a good quantitative fit for our data. This discrepancy can be resolved by mixing in a fraction of perpendicular dipoles. A dipoles distribution of 85% parallel and 15% perpendicular dipoles as shown in Fig. 13 gives a good fit, and is also consistent with the amplitude of the oscillation of the PL quantum efficiency (see Sec. III C 2). For an isotropic dipole distribution the average dipole moment would be given by 1/3 perpendicular and 2/3 parallel dipoles. The average dipole moment in our films therefore has a slightly larger parallel component than for the isotropic case. We consider that in our samples, which are prepared by spin coating, the polymer chains tend to align parallel to the substrate.

2. PL spectra and the branching ratio b

The magnitude of the oscillation of the PL quantum efficiency with distance between the emissive polymer film and the metal, as shown in Fig. 9, has another intriguing implication. As mentioned earlier, a change in PL efficiency due to interference effects can only occur when nonradiative decay channels from the same excited state as for the radiative decay compete with the radiative decay channels. Recently values varying from 0.1 to 1 have been reported for the branching ratio b [see Eq. (2)] in phenylene-vinylene polymers.[29,36–38] A low branching ratio means that the majority (a fraction of $1-b$) of the excitations formed from the initially excited state are nonemissive states. If the creation of nonemissive states is preferred to that of emissive excitons, the probability for radiative decay of the exciton has to be very high in order to achieve the overall PL quantum efficiencies typical of these materials. This means that the radiative rate has to be large compared to the nonradiative rate. However, we know that for the extreme case of the nonradiative rate being zero, the oscillation of the PL quantum efficiency as a function of the distance between the polymer and the metal film does not occur because of the lack of competition from nonradiative decay channels. We therefore expect the amplitude of the oscillation to be indicative of the branching ratio between purely nonemissive excited species and emissive excitons.

Using the simulated radiative power from a dipole in front of a mirror allows us to calculate the branching ratio b for the MEH-CN-PPV used in our experiments. From the simulations shown in Figs. 12 and 13, we calculated the ratio between the maximum radiative power for dipoles between 75 and 95 nm away from the metal and the minimum radiative power for the dipoles located at 210–230 nm from the metal. Taking the average over the luminescence spectrum (550–750 nm) weighted by the intensity of emission yields a ratio of 13 for parallel dipoles and 10 for the average orientation of the dipoles deduced above.

From the PL efficiency measurement (Fig. 9), we know that the maximum quantum efficiency corrected for the absorption of PL by the Al is 37%, and that the minimum quantum efficiency is 5.6%. The correction is necessary since the measured PL efficiency is not the PL quantum ef-

ficiency according to Eq. (2), but is modified by the absorption of PL by the metal. Inserting values for the radiative rate, the nonradiative rate and the branching ratio into Eq. (2), we can reproduce the amplitude of the oscillation in quantum efficiency, shown in Fig. 9, as a function of the ratio between the maximum and the minimum radiative rate and the branching ratio b.

If we choose the branching ratio to be 1 and the highest radiative rate in a way that the maximum quantum efficiency matches 37%, we obtain a minimum value for the PL quantum efficiency of 4.3% for parallel dipoles. A branching ratio of 0.5 yields a minimum PL efficiency of 9%. Taking the measured value of 5.6% (corrected for the absorption of light by the Al) for the minimum PL quantum efficiency gives a branching ratio of 0.7. For the case of a distribution of 85% parallel and 15% perpendicular dipole moments, the same analysis yields a branching ratio of 1. We note that the value of b calculated with the above method is highly sensitive to the dipole orientation. For an isotropic distribution of dipole moments we calculate an unphysical branching ratio b of 6.

We have also calculated a ratio of 10 between the maximum and the minimum radiative power of the dipoles from the experimentally deduced values for $g(\lambda)$ shown in Fig. 11. This reproduces the oscillation in quantum efficiency if the branching ratio b is 1. The calculation of the changes in radiative rate, $g(\lambda)$, due to interference is thus entirely consistent with the amplitude of the oscillation in PL quantum efficiency shown in Fig. 9, if the branching ratio is 1.

We note that the functions $g(\lambda)$ calculated with Eq. (7) and shown in Fig. 11 would be altered by the introduction of a branching ratio b of less than one since the efficiencies q_0 and q' in Eq. (7) would have to be substituted with q_0/b and q'/b. However, this would make the agreement between the simulations and the experimentally deduces curves of $g(\lambda)$ considerably worse.

From the above considerations and the evidence presented in Sec. III, we conclude that the branching ratio in our samples is close to 1 with the average dipole moment oriented slightly more parallel to the substrate than in the isotropic case. This is similar to previous estimates of the branching ratio in PPV based on the measurements of the PL quantum efficiency and PL decay times and the photovoltaic response of PPV/C_{60} photocells.[29,37,38] However, it has previously been speculated that in contrast to PPV the emissive species in the cyanoderivatives of PPV is not the same as initially photogenerated.[39,40] A high branching ratio then means that the conversion from the initially generated species to the emissive species is very efficient.

IV. EL DEVICES

A. PPV/MEH-CN-PPV double-layer LED's

Figure 14 shows the internal quantum efficiency of the PPV/MEH-CN-PPV double-layer devices as a function of the MEH-CN-PPV film thickness. The emission in these devices comes from the MEH-CN-PPV.[3,26,41] Fields of 5×10^5 V/cm were required to obtain current densities of 5 mA/cm^2. The internal quantum efficiency has been calculated from the light emitted into a collection angle of 24° in the forward direction, neglecting absorption in the device but allowing for refraction[42] and interference effects. Generally,

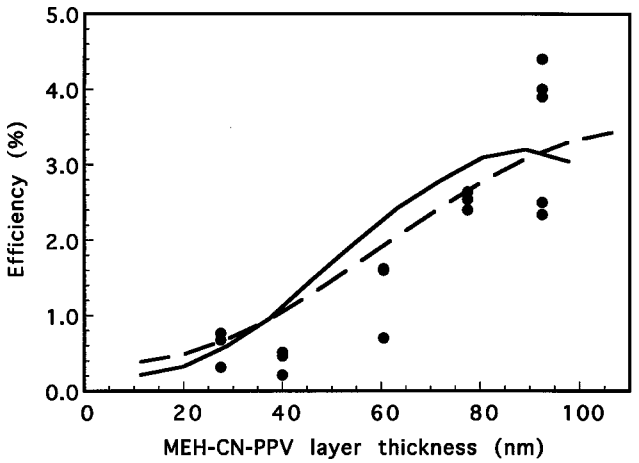

FIG. 14. Solid circles: Internal EL quantum efficiency for PPV/MEH-CN-PPV double layer devices as a function of the MEH-CN-PPV layer thickness. Measurements were made at current densities of 5 mA/cm^2. The EL efficiency was calculated taking the effects of interference on the angular dependence of the emission into account. The difference in optical path length due to the difference in refractive index between MEH-CN-PPV (1.7) and SiO_2 (1.47) was corrected for. The solid line shows a fit corresponding to a 20-nm-thick recombination zone at the polymer-polymer interface. The broken line shows a fit corresponding to a constant rate of formation of excitons throughout the thickness of the MEH-CN-PPV layer.

the correction that has to be made to account for the interference effects is dependent on the distance between the emitter and the metal film. However, it has been calculated that it is approximately constant for MEH-CN-PPV film thicknesses below 100 nm.[43] We note that if interference effects are neglected, as in Ref. 42, the internal quantum efficiencies are overestimated by about 40%. This may resolve some of the discrepancies found between the internal quantum efficiency and the total external quantum efficiency (including waveguided light) reported previously.[42] We note that the internal and the total external EL quantum efficiency should be identical if the absorption of light in the device is neglected.

In general, the EL quantum efficiencies obtained from double-layer devices exceed those from single-layer devices.[3,26,35,44] This improvement is believed to be due to three reasons.[3,34,44–46] Charge carriers are blocked by the band offset at the polymer-polymer interface, leading to an increased concentration of charge carriers at the interface and thus a narrower recombination zone. Accumulation of charge carriers at the interface causes a redistribution of the electric field, giving rise to enhanced electron injection and therefore a more balanced charge injection. Finally, the recombination zone is moved away from the metal interface, reducing nonradiative energy transfer to the metal and destructive interference due to the reflection of light by the metal. The relative importance of each of these effects for the increase in EL efficiency has been less clear. In PPV/MEH-CN-PPV double-layer devices, the electrons are blocked at the polymer-polymer interface, whereas holes are injected from the PPV into the MEH-CN-PPV, where an exciton can then be generated; hence the emission in these devices comes from the MEH-CN-PPV. As a result holes, which are the

majority charge carriers in single-layer PPV devices, cannot travel to the Al electrode, and exciton formation close to the Al is reduced.

The EL efficiency of the devices increases with MEH-CN-PPV layer thickness. The dependence of the EL efficiency on the MEH-CN-PPV film thickness is similar to that of the PL efficiency shown in Fig. 9. Since in our materials the same emissive species is responsible for EL and PL, we expect the Al film to influence the EL efficiency in the same way as shown for the case of PL.[47] In other words, the effects of nonradiative energy transfer and interference on the efficiency for radiative emission from singlet excitons should be identical to the effects described for PL. In our devices the MEH-CN-PPV layer thickness determines the distance between the emitting dipoles and the metal electrode. Our results show that the removal of the recombination zone from the metal interface is crucial to the improved EL efficiencies seen in double-layer devices. Figure 14 also shows two fits to the EL quantum efficiency data, obtained from using the dependence of the PL quantum efficiency of a 20-nm-thick MEH-CN-PPV layer on the distance between the polymer film and an Al film (see Fig. 9). The solid line corresponds to a 20-nm-thick recombination zone in the MEH-CN-PPV layer at the polymer-polymer interface. The broken line corresponds to a case where electron-hole capture occurs uniformly throughout the MEH-CN-PPV film. As expected, the EL data follow the trend of the two fits. It appears that the second fit agrees slightly better with the EL quantum efficiency data than the first. However, both fits underestimate the reduction of electroluminescence with decreasing MEH-CN-PPV film thickness. We consider that the passage of holes through thin MEH-CN-PPV layers without recombination will also contribute to the reduction of EL. Because of this additional process and the noise in the EL data, the dependence of the EL quantum efficiency on the MEH-CN-PPV layer does not give conclusive information about the extent of the recombination zone.

Since we have measured the PL quantum efficiency as a function of distance from a metal electrode, we can predict the efficiency of radiative decay of singlet excitons in LED's as a function of the distribution of exciton formation in the device. The fits shown in Fig. 14 were scaled with respect to the PL efficiency data shown in Fig. 9. If all injected charges recombine within the device, we expect the scaling factor to be 1/4, due to spin degeneracy.[25] For the fit corresponding to a 20-nm-thick recombination zone at the polymer-polymer interface we require a scaling factor of 1/11. However, for a uniform distribution of excitons formed in the MEH-CN-PPV layer the scaling factor was only $1/(5.5)$, since some of the excitons are generated close to the Al, where they are quenched effectively. Clearly, the further the recombination zone extend toward the Al, the lower the probability of radiative decay. To achieve a certain EL quantum efficiency this requires that a higher fraction of injected charges recombine. We note that for the most efficient device measured a uniform distribution of exciton formation would require a fraction of injected charges recombining to form singlet excitons which is greater than 1/4. We therefore conclude that the distribution of exciton formation is weighted toward the polymer-polymer interface. This is analogous to the situation observed in molecular organic LED's.[45,48]

B. Design rules for LED's and photovoltaic cells

In the following we propose design rules for LEDs and photovoltaic cells geared to increase their efficiencies. As seen from the oscillations in Figs. 9 and 11–13, constructive interference can be a powerful tool to improve the radiative rate of an emitter in front of a reflective metal surface. Optimizing the device structure and possibly the alignment of the polymers can therefore considerably improve the quantum efficiency of a light-emitting device with a similar structure. A large dependence of the EL efficiency on the distance between a metal electrode and the emission layer and changes in the EL spectra due to interference effects have been observed in molecular organic LED's.[34,44,48] In order to maximize the EL quantum efficiency of a LED, the emission should come from a region where nonradiative energy transfer to a metal electrode is minimal, and the radiative rate averaged over the emission spectrum and all directions is maximal as a result of constructive interference. The optimum position of the emission region depends on the orientation of the average dipole moment. Double-layer devices offer the possibility to locate the emission at a distance where the above conditions are fulfilled.

For metal electrodes nonradiative energy transfer in the visible becomes negligible for distances larger than $(90/n)$ nm, where n is the refractive index of the medium separating the emitter from the metal. From the simulations of the radiative power we conclude that the maximum radiative rate for emission in the visible integrated over all angles is obtained for parallel dipoles within a 20-nm-thick MEH-CN-PPV film at a distance from the metal of approximately

$$d = 0.33\left(\frac{\lambda}{n}\right) - 54 \text{ nm}, \tag{9}$$

where d is the distance in nm, λ is the weighted average emission wavelength in nm, and n is the refractive index of SiO_2. We confirmed this result for the PL from a MEH-CN-PPV film separated from the metal by SiO_2. With an emission centered around 600 nm, and a refractive index for SiO_2 of 1.47, we calculate an optimum distance of 80 nm. This is close to the 75 nm for which the maximum PL efficiency was measured. We note that the optimum distance between the emitter and the metal depends on the phase change on reflection from the metal, all interfaces in the device structure, and the emission angle.

Our results also have implications for photovoltaic devices. In photovoltaic devices light is absorbed and electron-hole pairs are created in the device. The electron and hole then have to be separated and collected at opposite electrodes. If highly luminescent materials are used as absorbing layers, e.g., MEH-PPV or MEH-CN-PPV, radiative recombination of an exciton is an efficient loss mechanism as it reduces the number of charges available to be collected at the electrodes. The suppression of light emission due to interference effects allows us to reduce these losses. If the radiative lifetime is enhanced as a consequence of destructive interference due to reflection of light from a mirror in the device, the lifetime of the exciton and therefore the probability of successful charge separation is increased. The design goals for photovoltaic device structures are therefore in some ways the opposite of those for LED's. Most of the light should be

absorbed, and thus excitons created in a region where the luminescence efficiency is low, yet nonradiative energy transfer has to be avoided since it acts as a quenching mechanism without separating the charges. However, the suppression of light emission in photovoltaic devices seems to have a serious drawback. The metal electrode will modify the absorption in the same fashion as the emission coefficient, leading to a low absorption coefficient in the wavelength range of the emission. However, light emission occurs at lower energies than the absorption, and the overlap between the absorption and emission spectra in conjugated polymers is typically very small. This allows a device design for which the active layer of the photovoltaic cell is in a region where the radiative rate is low in the emission range but high in the wavelength range where the material absorbs.

The ideal position for light absorption in a MEH-CN-PPV single-layer device would therefore be around 220 nm from the metal. Selecting this region could be achieved by illuminating the 240-nm-thick device through an ITO electrode. If thinner polymer films are preferred, a transparent electron transport layer can be used in order to achieve the optimum separation between the polymer film and the Al.

V. COMMENTS ON PREVIOUS WORK

A. Exciton diffusion length and exciton quenching

Other workers have attempted to extract values for the exciton diffusion range by considering quenching of excitons after diffusion to a Ca interface.[28] It was assumed that exciton quenching occurs only when the exciton diffuses to the Ca interface. An estimate of the exciton diffusion range in phenylene vinylene oligomers of 20 nm was obtained.

Our results demonstrate that efficient quenching of PL and EL due to nonradiative energy transfer occurs within a distance of 60 nm from the metal, substantially reducing the quantum efficiency of the emitting polymer. It occurs even when the polymer is separated from the metal by a transparent spacer layer, and it does not require direct contact between the exciton and the metal. For this reason great caution should be taken in attempting to deduce the diffusion range of the exciton from such experiments.

B. Polymer-metal interface formation

Chemical interactions at the interface between PPV and metal electrodes have been proposed to explain the changes in the EL and PL spectra for different device structures.[49] It is concluded that the further away from the metal the emission occurs, the smaller the changes in the emission spectrum are. The shape of the emission spectra depends also on the metal electrode used. The authors neglect interference effects as a possible explanation, since no dependence of the emission color on viewing angle was observed. Our results show that interference between the directly emitted and the reflected waves has a pronounced effect on the shape of the emission spectra in different device structures. Figures 6 and 10 show the changes in the PL spectra of MEH-CN-PPV as a function of polymer layer thickness or polymer metal film separation. In the latter case no contact between the polymer and the metal is made. Therefore the changes in emission cannot be due to a chemical reaction between the polymer and the metal. The comparison of the radiative rates deduced from the measured spectra and the simulations shown in Figs. 12 and 13 also demonstrates that the shapes of the emission spectra can be satisfactorily explained simply by considering interference effects.

VI. CONCLUSION

Our results clearly show that the presence of a metal film has a pronounced effect on the PL and EL quantum efficiency, and the shape of the emission spectra from light-emitting polymer devices. We have shown that the effects of interference on the radiative rate and nonradiative energy transfer to the metal on the nonradiative rate can fully explain these results. These effects have to be taken into account in a variety of experiments in which they have often been neglected in the past. They also allow us to optimize the design of light-emitting or light-absorbing devices such as LED's and photovoltaic cells. By avoiding nonradiative energy transfer to the metal and making optimum use of interference effects due to the metal layer, the efficiency of light emission can be significantly enhanced. The position of the emission region relative to the metal film can also be used to modify the emission spectrum of a device. We have shown that the removal of the recombination zone from the metal electrode is crucial to the increased EL efficiency of PPV/MEH-CN-PPV double-layer devices.

In addition, our measurements of the PL quantum efficiency of a polymer film in front of a metal film served as a measurement of the orientation of the dipoles in the polymer film and the branching ratio in conjugated polymers. For such measurements conjugated polymers are suitable materials, since they allow one to probe a large part of the visible spectrum with just one emissive material because of their broad emission. We have deduced that the orientation of the dipoles in MEH-CN-PPV deviates slightly from an isotropic distribution. As a result of the spin-coating process the dipole moment tends to lie parallel to the substrate. The branching ratio for MEH-CN-PPV was found to be close to 1.

ACKNOWLEDGMENTS

We thank N. C. Greenham and N. Tessler for useful discussions, and Cambridge Display Technology for the supply of the materials.

[1] J. H. Burroughes, D. D. C. Bradley, A. R. Brown, R. N. Marks, K. Mackay, R. H. Friend, P. L. Burn, and A. B. Holmes, Nature (London) **347**, 539 (1990).

[2] D. Braun and A. J. Heeger, Appl. Phys. Lett. **58**, 1982 (1991).

[3] N. C. Greenham, S. C. Moratti, D. D. C. Bradley, R. H. Friend, and A. B. Holmes, Nature (London) **365**, 628 (1993).

[4] I. D. W. Samuel, B. Crystall, G. Rumbles, P. L. Burn, A. B. Holmes, and R. H. Friend, Chem. Phys. Lett. **213**, 472 (1993).

[5] Q. Pei, G. Yu, C. Zhang, Y. Yang, and A. J. Heeger, Science **269**, 1086 (1995).
[6] R. N. Marks, J. J. M. Halls, D. D. C. Bradley, R. H. Friend, and A. B. Holmes, J. Phys. Condens. Matter. **6**, 1379 (1994).
[7] N. Tessler, G. J. Denton, and R. H. Friend, Nature (London) **382**, 695 (1996).
[8] U. Lemmer, R. Hennig, and W. Guss *et al.*, Appl. Phys. Lett. **66**, 1301 (1995).
[9] H. F. Wittmann, J. Grüner, R. H. Friend, G. W. C. Spencer, S. C. Moratti, and A. B. Holmes, Adv. Mater. **6**, 541 (1995).
[10] A. Dodabalapur, L. J. Rothberg, R. H. Jordan, T. M. Miller, R. E. Slusher, and J. M. Phillips, J. Appl. Phys. **80**, 6954 (1996).
[11] S. E. Burns, N. Pfeffer, J. Grüner, M. Remmers, T. Javoreck, D. Neher, and R. H. Friend, Adv. Mater. **9**, 395 (1997).
[12] D. G. Lidzey, M. A. Pate, D. M. Whittaker, D. D. C. Bradley, M. S. Weaver, T. A. Fisher, and M. S. Skolnick, Chem. Phys. Lett. **263**, 655 (1996).
[13] H. Morawitz, Phys. Rev. **187**, 1792 (1969).
[14] H. Kuhn, J. Chem. Phys. **53**, 101 (1970).
[15] K. H. Drexhage, in *Progress in Optics*, edited by E. Wolf (North-Holland, Amsterdam, 1974), pp. 163–232.
[16] R. R. Chance, A. Prock, and R. Silbey, J. Chem. Phys. **60**, 2744 (1974).
[17] R. R. Chance, A. Prock, and R. Silbey, J. Chem. Phys. **60**, 2184 (1974); **60**, 2185 (1974).
[18] R. R. Chance, A. Prock, and R. Silbey, J. Chem. Phys. **62**, 2245 (1975).
[19] R. R. Chance, A. Prock, and R. Silbey, Adv. Chem. Phys. **37**, 1 (1978).
[20] E. A. Hinds, in *Cavity Quantum Electrodynamics*, edited by P. R. Berman (Academic, San Diego, 1994).
[21] B. N. J. Persson and N. D. Lang, Phys. Rev. B **26**, 5409 (1982).
[22] G. Cnossen, K. E. Drabe, and D. A. Wiersma, J. Chem. Phys. **98**, 5276 (1993).
[23] T. Tsutsui, C. Adachi, S. Saito, M. Watanabe, and M. Koishi, Chem. Phys. Lett. **182**, 143 (1991).
[24] S. E. Burns, N. C. Greenham, and R. H. Friend, Synth. Met. **76**, 205 (1996).
[25] A. R. Brown, J. H. Burroughes, N. Greenham, R. H. Friend, D. D. C. Bradley, P. L. Burn, A. Kraft, and A. B. Holmes, Appl. Phys. Lett. **61**, 2793 (1992).
[26] D. R. Baigent, N. C. Greenham, J. Grüner, R. N. Marks, R. H. Friend, S. C. Moratti, and A. B. Holmes, Synth. Met. **67**, 3 (1994).
[27] J. Bigerson, M. Fahlman, P. Bröms, and W. R. Salaneck, Synth. Met. **80**, 125 (1996).
[28] V. Choong, Y. Park, and Y. Gao, Appl. Phys. Lett. **69**, 1492 (1996).
[29] N. C. Greenham, I. D. W. Samuel, G. R. Hayes, R. T. Phillips, Y. A. R. R. Kessener, S. C. Moratti, A. B. Holmes, and R. H. Friend, Chem. Phys. Lett. **241**, 89 (1995).
[30] J. C. deMello, H. F. Wittmann, and R. H. Friend, Adv. Mater. **9**, 230 (1997).
[31] E. D. Palik, *Handbook of Optical Constants of Solids* (Academic Press, London, 1991).
[32] R. W. Gymer (private communication).
[33] H. Becker, S. E. Burns, N. Tessler, and R. H. Friend, J. Appl. Phys. **81**, 2825 (1996).
[34] S. Saito, T. Tsutsui, M. Era, N. Takada, E. Aminaka, and T. Wakimoto, Mol. Cryst. Liq. Cryst. **253**, 125 (1994).
[35] C. Adachi, T. Tsutsui, and S. Saito, Appl. Phys. Lett. **57**, 531 (1990).
[36] L. J. Rothberg, M. Yan, F. Papadimitrakopoulos, M. E. Galvin, E. W. Kwock, and T. M. Miller, Synth. Met. **80**, 41 (1996).
[37] J. J. M. Halls, K. Pichler, R. H. Friend, S. C. Moratti, and A. B. Holmes, Appl. Phys. Lett. **68**, 3120 (1996).
[38] N. T. Harrison, D. R. Baigent, G. R. Hayes, R. T. Phillips, and R. H. Friend, Phys. Rev. Lett. **77**, 1881 (1996).
[39] I. D. W. Samuel, G. Rumbles, and C. J. Collison, Phys. Rev. B **52**, 11 573 (1995).
[40] D. R. Baigent, A. B. Holmes, S. C. Moratti, and R. H. Friend, Synth. Met. **80**, 119 (1996).
[41] N. C. Greenham, J. Shinar, J. Partree, P. A. Lane, O. Amir, F. Lu, and R. H. Friend, Phys. Rev. B **53**, 13 528 (1996).
[42] N. C. Greenham, R. H. Friend, and D. D. C. Bradley, Adv. Mater. **6**, 491 (1994).
[43] N. Tessler (private communication).
[44] C. W. Tang and S. A. VanSlyke, Appl. Phys. Lett. **51**, 913 (1987).
[45] C. W. Tang, S. A. VanSlyke, and C. H. Chen, J. Appl. Phys. **65**, 3610 (1989).
[46] D. V. Khramtchenkov, H. Bässler, and V. I. Arkhipov, J. Appl. Phys. **79**, 9283 (1996).
[47] J. Salbeck, Ber. Bunsenges. Phys. Chem. **100**, 1667 (1996).
[48] C. Adachi, T. Tsutsui, and S. Saito, Acta Polytech. Scand. Appl. Phys. **170**, 215 (1990).
[49] J. Peng, B.-Y. Yu, C.-H. Pyun, C.-H. Kim, K.-Y. Kim, and J.-I. Jin, Jpn. J. Appl. Phys. **35**, L317 (1996).